Interannual Variability and Climatic Noise in Satellite-Observed Outgoing Longwave Radiation

DAVID A. SHORT AND ROBERT F. CAHALAN

Laboratory for Atmospheric Sciences, Goddard Space Flight Center, Greenbelt, MD 20771

(Manuscript received 12 August 1982, in final form 21 December 1982)

ABSTRACT

The interannual variability (IAV) in monthly averaged outgoing infrared radiation (IR, from the NOAA polar orbiting satellites) is observed to be larger during summer than during winter over the north Pacific Ocean. A statistical analysis of the daily observations shows the daily variance to be similar during both seasons while the autocorrelation function is quite different. This leads to a seasonal difference in estimates of the climatic noise level, i.e., the variances expected in summer and winter monthly averages due to the number of effectively independent samples in each average. Because of a less vigorous tropospheric circulation, monthly means of IR during summer are affected by the passage of fewer synoptic-scale disturbances and their attendant cloudiness. Fewer independent samples imply a larger variance in the time averages. While the observed IAV is less in winter, the ratio of the observed IAV to the climatic noise level is larger, suggesting that signals of climatic variability in outgoing IR may be more readily diagnosed during winter in this region. The climatic noise level in monthly averaged IR and cloudiness is also estimated for two other climatic regimes—the quiescent subtropical north Pacific and the ITCZ in the western Pacific.

1. Introduction

Since 1974, measurements of outgoing longwave radiation (IR), made twice daily from scanning radiometers aboard the polar orbiting series NOAA-3, 4, 5 and 6 and TIROS-N, have been archived and made available in convenient form by the National Environmental Satellite Data Information Service (NESDIS) of NOAA (Gruber and Winston, 1978). This long time series of IR observations, with global coverage, is particularly interesting because it permits stable estimates of the statistics of short time scale fluctuations, dominated by variations in cloudiness (Cahalan *et al.*, 1982, hereafter referred to as CSN), as well as some insight into longer time scale phenomena [the annual cycle and interannual variability as explored by Heddinghaus and Krueger (1981) and Liebmann and Hartmann (1982)]. Interannual variability (IAV) in meteorological data is typically examined in monthly averages with the annual cycle removed. In such finite time averages a certain amount of IAV is associated with the limited sample. This climatic noise (Leith, 1973) is due to the unpredictable nature of short-term fluctuations (weather) and cannot be eliminated by measuring continuously with an error-free observing system. An estimate of the climatic noise, also referred to as natural variability (Madden, 1976), in meteorological fields can be made from the variance and autocorrelation statistics of the day-to-day observations. It is then of interest to identify geographic regions where the observed IAV is much larger than the climatic noise. These regions can be examined in greater detail in hopes of clearly diagnosing signals of short-term climatic variability (such as the Southern Oscillation/El Niño phenomena). The observed IAV and estimates of the climatic noise level for surface pressure and surface temperature have been mapped from time series of surface station observations which are much longer than those currently available from satellites (e.g., Madden, 1976; Madden and Shea, 1978).

It is the purpose of this contribution to make an estimate of the climatic noise level in satellite observed IR for several climatic regimes over the Pacific Ocean. We have chosen regions where the diurnal cycle in cloudiness and surface temperature has only a small influence on the IR (Short and Wallace, 1980) and its autocorrelation function. This is because the diurnal cycle is not yet understood in sufficient detail to remove its effects, whereas the short autocorrelation times of the IR signal require observations at intervals of less than one day in order to accurately represent their structure (CSN). Over the North Pacific Ocean we demonstrate a strong seasonal modulation in both the climatic noise level and observed interannual variability. This seasonal modulation of the climatic noise is due to a change in the position and intensity of the midlatitude storm track over the course of the year (CSN, especially Figs. 10a and 10b).

The climatic noise level in meteorological data may depend on the size of the area over which the measurements are averaged. Typically we see less daily variance and longer autocorrelation times for larger areal averages. An examination of the averaging area

dependence of climatic noise in this type of data is presented as guidance for the space–time sampling strategies of future climate observing systems.

2. Data

The values of total outgoing longwave radiation (IR) used in this study were derived from measurements taken by scanning radiometers aboard the NOAA polar orbiter series (NOAA-3, 4, 5, 6 and TIROS-N) during the periods June 1974 to February 1978 and January 1979 to February 1981, inclusive. The infrared sensors detect upwelling radiation twice daily over all areas of the globe in the 10.5–12.5 μm wavelength band (the water vapor window), where variations are caused mainly by clouds within the field of view. We feel confident that our analysis of this long time series is not seriously affected by calibration or instrument degradation problems because the globally averaged IR does not show long-term trends or discontinuities (Lau, private communication, 1982). Scene-to-scene variations in the inferred outgoing IR are 10–100 times larger than the 1 W m^{-2} uncertainty introduced by instrument noise.

The original 4–8 km resolution measurements have been spatially averaged to a resolution of 2½° of latitude by 2½° of longitude on a global grid and made available on digital tape by the National Environmental Satellite Data Information Service of NOAA (Gruber and Winston, 1978).

For the purposes of this study we will concentrate on a portion of the Pacific Ocean where previous work has focused on the day-to-day variability in IR associated with the passage of synoptic-scale weather disturbances and their cloud systems (Reed, 1979; CSN). For a detailed description of the daily and seasonal variability in these data the reader is referred to CSN.

3. Climatic noise and observed interannual variability

Interannual variability of the January IR was determined by computing the mean of the available Januarys and then finding the deviation of the individual January means from that mean. The same procedure was followed for each month (using 30 daytime periods beginning with the first day of the month). Fig. 1a is a histogram of monthly mean anomalies for winter months (6 Decembers, 6 Januarys, 6 Februarys) at 14 gridpoints over the North Pacific (150°E–150°W, every 10° at 42.5°N and 37.5°N). The 14 gridpoints are spaced such that their daily fluctuations are essentially independent but have nearly identical lag autocovariances. By compositing data from these gridpoints we can increase the size of our sample and obtain distributions of anomalies which are as smooth as one would expect from a long time series of observations. This region was chosen because earlier analyses (Lau, 1978; CSN,

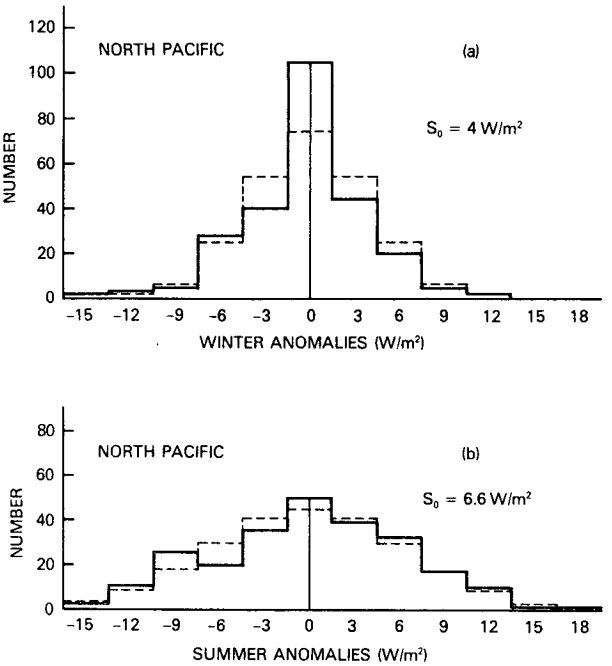

FIG. 1. Monthly mean IR anomalies at 14 grid boxes (2½° × 2½° each) over the North Pacific (centered 150°E to 150°W, every 10°, at 37.5°N and 42.5°N) from the period June 1974 to February 1981. (a) Winter anomalies from 6 Decembers, 6 Januarys and 6 Februarys. (b) Summer anomalies from 6 Junes, 6 Julys and 6 Augusts. Dashed lines represent normal distributions with the same variance (S_0) as the observed distributions.

1982; White, 1982) indicated that the winter storm track goes right through it, while during summer the storm track is weaker and farther north. IAV during summer months (Fig. 1b) is considerably larger. Both distributions are approximately normal, and it is estimated that there is less than a 1% chance that they were drawn from the same population.[1]

The primary question of this paper is, "How large must these anomalies be before we can reject the null hypothesis that they are due to the limited sample in the monthly mean?" The daily variance in the observations is approximately the same during winter and summer, so that the crudest estimate for sampling fluctuations, the familiar $1/N^{1/2}$ law for independent observations, would yield the same noise level in both seasons. However, when we take account of the correlation between consecutive observations, we shall see that the noise is so much smaller in winter that, in spite of the smaller variability seen in Fig. 1a

[1] This is based on Fisher's F distribution. Degrees of freedom (dof) were estimated to be ~50 by assuming two or three independent areas within the region for each of the 18 months. We know that adjacent gridpoints are highly correlated on the daily time scale and even more so on the monthly time scale due partly to the advecting short-term correlations. The statistical significance is not sensitive to this dof assumption.

than in 1b, a greater fraction of anomalies are significant in winter.

Using the statistical theory of sampling we can estimate the climatic noise level from the variance and autocorrelation of the observations. Let X_k (k = 1, 2, . . . , n) be a set of n observations during a given month, and let $\bar{X}_T$ denote the monthly mean, so that

$$\bar{X}_T = \frac{1}{n}\sum_{k=1}^{n} X_k. \quad (1)$$

For twice daily observations k runs from 1 to 60. Then the expected variance in the monthly means is given by (Jones, 1975)

$$\mathrm{Var}(\bar{X}_T) = \frac{S_D^2}{n}\left[1 + 2\sum_{\tau=1}^{n-1}\left(1 - \frac{\tau}{n}\right)R_X(\tau)\right], \quad (2)$$

where here τ is in units of the sampling interval. The variance S_D of the observations can be written

$$S_D^2 = \frac{1}{(n-1)}\sum_{k=1}^{n}(X_k - \bar{X}_T)^2, \quad (3)$$

while

$$R_X(\tau) = \frac{1}{(n-\tau)}\sum_{k=1}^{n-\tau}(X_k - \bar{X}_T)(X_{k+\tau} - \bar{X}_T)/S_D^2 \quad (4)$$

is the autocorrelation of the observations. This analysis assumes that the twice daily observations are equally spaced in time. In reality the geometry of the polar orbiter data swaths causes the interval between observations over a point to vary from 11 to 13 h. In the storm track region where the signal varies quite rapidly, we estimate that this timing factor introduces at most an effective 10 W m^{-2} uncertainty. Thus the variance from (3) is slightly overestimated, while the autocorrelation from (4) is slightly underestimated. The net effect on estimates of the climatic noise from (2) is insignificant.

Time series of IR from which $R(\tau)$ were computed are approximately stationary (see CSN, Fig. 2). Small contributions to the variance from the seasonal cycle have been removed by a least-squares quadratic fit. From (2) we see that the expected variance in monthly means is determined by the character of day-to-day changes as reflected in the observations. If the observations were uncorrelated [$R(\tau) = 0$] then $\mathrm{Var}(\bar{X}_T)$ would depend only on the number of observations used to determine $\bar{X}_T$. The *effective* number of independent observations depends on the summation term in (2). Consecutive observations are correlated in a manner which can be thought of as depending upon the typical size, speed and lifetime of passing weather disturbances. During summer, because the disturbances move more slowly, there are fewer independent samples and therefore a greater variance in the monthly means. Sampling fluctuations in monthly averaged IR, due to variations in the number or intensity of storm events from one summer to another, would take place even in the absence of climatic trends or short-term climatic variations.

Autocorrelation functions for the winter and summer months over the central North Pacific, as determined from twice daily observations, are shown in Fig. 2. The rapid decrease of correlation with time during winter is caused by rapidly moving weather systems in the region. The negative correlation peak is associated with an eastward shift of the east/west, cloudy/clear pattern accompanying baroclinic disturbances in the westerlies (see CSN, Figs. 7a, b). Notice that the daily variance [S_D in (2)] is approximately the same during winter and summer. The magnitude of the climatic noise level for each calendar month as computed from (2) involves values of the autocorrelation at various lag times τ. Contributions to (2) are negligible beyond three days (see CSN, Fig. 5a) where $R(\tau)$ begins to behave as one would expect from a finite sample estimation. Namely, small fluctuations about zero which increase in amplitude as the overlap between the time series and its lagged counterpart is decreased. As more satellite data become available we should be able to confidently interpret small variations in $R(\tau)$ at longer lags and incorporate their effects on estimates of the climatic noise.

The expected IAV ($\mathrm{Var}(\bar{X}_T)$) during summer as computed from (2) is (4 W m^{-2})^2, whereas during winter it is only (2 W m^{-2})^2. The ratio of the observed IAV to the climatic noise is 2.7 during summer and 4.0 during winter [using S_0^2 from Fig. 1 and $\mathrm{Var}(\bar{X}_T)$ from (2)]. Both ratios are statistically significant at the 95% level (again using Fisher's F distribution).

These ratios suggest that signals of short-term climatic variability (such as persistent sea surface temperature anomalies and/or large-scale atmospheric circulation anomalies) are responsible for a larger fraction of IAV in monthly averaged IR during winter than during summer.

By compositing monthly mean anomalies from

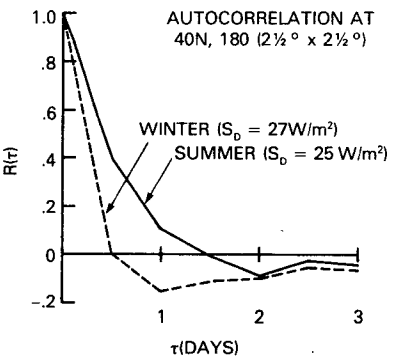

FIG. 2. Autocorrelation functions of IR at 40°N, 180 (2½° × 2½° resolution) for winter (DJF) and summer (JJA) months.

many gridpoints we have been able to construct the fairly smooth distributions of Fig. 1 and understand their differences. While the distribution of anomalies from a single gridpoint is by necessity much noisier, it is instructive to examine such a distribution together with its climatic noise confidence limits. Fig. 3 shows the monthly mean IR anomalies at 40°N, 180° along with a curve of the 95% confidence interval for each month of the year. In the absence of short-term climatic variability we would expect 95% of the anomalies to be inside the $\pm 2\mathrm{Var}(\bar{X}_T)^{1/2}$ bounds. More than 25% of the anomalies are outside the bounds. A χ^2 test on the distribution of anomalies normalized with respect to their noise level shows this result to be significant at the 99% level. The largest anomaly (with respect to the climatic noise level) occurs in January 1977. This anomaly of -9 W m^{-2} is associated with an anomalous circulation pattern in which a strong ridge over the west coast of North America was flanked by deep troughs over the North Pacific and the eastern United States (where record cold temperatures were observed). A similar pattern was also observed in January of 1981 (the -8 W m^{-2} anomaly in Fig. 3).

Further studies of this type of data promise to add more information on the morphology of signals of short-term climatic variability and patterns of atmospheric teleconnections [Wallace and Gutzler (1981) and Horel and Wallace (1981) provide extensive reference lists on teleconnection studies]. The Southern Oscillation/El Niño phenomenon is a signal of short-term climatic variability which is readily apparent in tropical cloudiness and IR fields (see, e.g., Heddinghaus and Krueger, 1981; Liebmann and Hartmann, 1982). Its influence on midlatitude cloudiness is more subtle. As more satellite data become available, we may be able to apply more sophisticated signal processing techniques in order to separate signals of short-term climatic variability from climatic noise (as suggested by Hasselmann, 1979; Madden, 1981; and Bell, 1982).

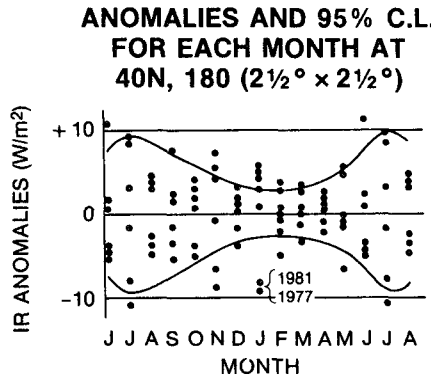

FIG. 3. Anomalies in monthly mean outgoing IR for each month. Thin line envelope is the 95% confidence level of "climatic noise" as explained in the text.

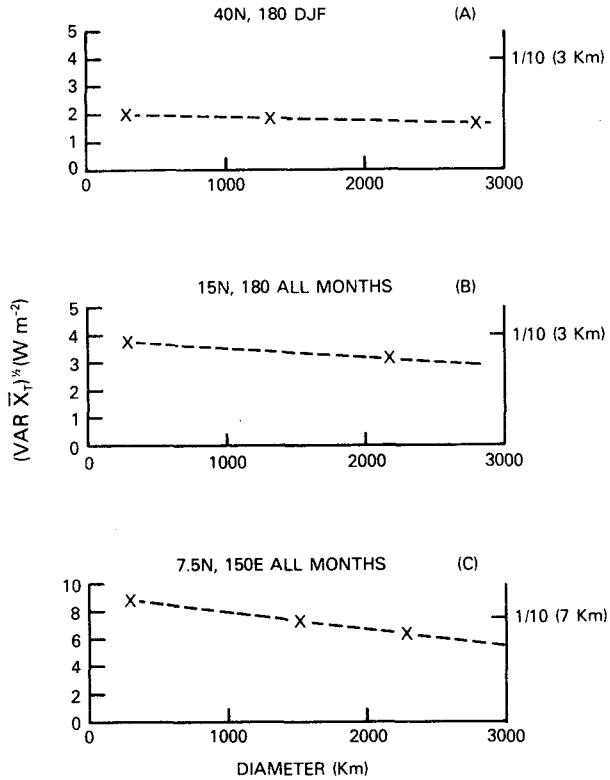

FIG. 4. Estimated climatic noise levels versus diameter of averaging area. Left scale is for IR, right is for cloud cover, with assumed cloud top height in parentheses. Averaging areas are centered at (a) 40°N, 180°, (b) 15°N, 180° and (c) 7.5°N, 150°E.

4. Area-averaging effects

Just as time averaging reduces the climatic noise level [the $1/n$ factor in (2)] we might expect that averaging observations over a larger spatial area would achieve the same effect. However, noise reduction by spatial averaging is mitigated by the fact that, while there is less daily variance for larger spatial averages, the autocorrelation shows more persistence. The two effects tend to cancel one another, causing the climatic noise level to decrease slowly as averaging area is increased. [A simple stochastic model illustrating the two effects is described in Cahalan (1981).]

Fig. 4 shows the estimated climatic noise level in three climatic regimes for averaging areas with effective diameters of ~250 km (2½° × 2½°) out to effective diameters of 3000 km. This range includes averaging areas typically used in data sets for climatic research as well as those equivalent to the field of view observed by medium and wide field of view radiometers aboard low earth-orbiting satellites.

Climatic noise levels for each regime were estimated for the 2½° × 2½° grid boxes provided by NESDIS as well as for averages over areas one "correlation diameter" across (see CSN). These effective correlation diameters are ~1300, 2200 and 1500 km over the North, central and equatorial Pacific, re-

spectively. As the averaging area was further increased, it was found that the climatic noise level could be approximated as the noise level of the area one correlation diameter across, divided by the number of effectively independent samples within the area (as determined by the correlation diameter). The noise level over the quiescent subtropical Pacific (Fig. 4b) is larger than over the winter storm track because of a longer autocorrelation time. Var(X_T) was computed using lags out to five days for Figs. 4b and 4c. Over the ITCZ (Fig. 4c) the daily variance and autocorrelation time are both larger than for Fig. 4a, giving the largest noise level.

By assuming an average effective cloud top height for the regions having IR noise levels represented in Fig. 4, the corresponding noise levels in cloud coverage can be estimated. For 3 km cloud tops the cloud top temperature would be ~20°C colder than the surface and the outgoing IR would be ~40 W m^{-2} less, or 4 W m^{-2} per tenth cloud cover. [The approximate relationship of $\Delta IR/\Delta T \approx 2$ W m^{-2} (C°)$^{-1}$ is discussed in CSN.] The right-hand vertical scales in Figs. 3a–c are labeled as cloud amount variability equivalent to the IR variability for that regime (with assumed effective cloud top height in parentheses). The estimated climatic noise level in cloud amount is smallest over the midlatitude region and approximately equal for the two tropical regimes.

5. Discussion

Our main conclusions are as follows:

1) In spite of the fact that the monthly averaged IR in the midlatitude storm track is less variable in winter than summer, a greater fraction of the IR anomalies are statistically significant in winter because of the smaller climatic noise level. The smaller wintertime climatic noise is not due to decreased daily variance, but rather to shorter autocorrelation times. The largest anomalies, with respect to the climatic noise level, occur during winter. January 1977 is discussed as an example of an extreme IR anomaly which is associated with an anomalous atmospheric circulation pattern. The climatic noise level is largest over the ITCZ due to the high daily variance and relatively long autocorrelation time.

2) It appears that the climatic noise level in IR and cloudiness does not decrease rapidly as averaging area is increased. While averaging over large areas may be suitable for detecting global or hemispheric signals of climatic variability (Bell, 1982), such a procedure may erode information about the spatial structure of climatic anomalies. Continuing archives of satellite data having a spatial resolution comparable to or better than present operational models of the general circulation is clearly important. Diagnostic studies of these global data bases promise to add to our understanding of the morphology of, evolution of, and dynamical forcings responsible for signals of short-term climatic variability.

While the present study has focused on the expected variance of time averages, a natural next step will be an examination of the expected covariance or correlation of time averages. Using X and Y to denote two gridpoints and using the notation of Section 3, the expected correlation of time averages at the two points is given by

$$R_{\bar{X}_T\bar{Y}_T}(0) = \frac{\mathrm{Cov}(\bar{X}_T, \bar{Y}_T)}{[\mathrm{Var}(\bar{X}_T)]^{1/2}[\mathrm{Var}(\bar{Y}_T)]^{1/2}} = \frac{R_{XY}(0) + \sum_{\tau=1}^{n-1}\left(1-\frac{\tau}{n}\right)R_{XY}(\tau) + \sum_{\tau=1}^{n-1}\left(1-\frac{\tau}{n}\right)R_{XY}(-\tau)}{\left[1+2\sum_{\tau=1}^{n-1}\left(1-\frac{\tau}{n}\right)R_X(\tau)\right]^{1/2}\left[1+2\sum_{\tau=1}^{n-1}\left(1-\frac{\tau}{n}\right)R_Y(\tau)\right]^{1/2}}. \quad (5)$$

Here $R_{XY}(\tau)$ is the cross correlation of the observations at lag τ, and $T = n\Delta t$ is the length of the time average, where Δt is the time interval between observations.

Teleconnection studies often present maps of the covariance or correlation of monthly averaged anomalies between one gridpoint and all others. Instantaneous observations at nearby gridpoints are correlated because of the finite size of weather disturbances. Monthly averages will tend to be more highly correlated in the preferred direction of movement of the disturbances because of their finite lifetimes. The role of advecting short-term correlations in determining the shape of time-averaged correlation fields can be clearly demonstrated with a simple stochastic model (Cahalan, 1981). Their influence also appears to be manifested by an east–west elongation in correlation fields of geopotential height along the axes of major jet streams (see, e.g., Wallace and Gutzler, 1981, Fig. 24b). A more complete understanding of teleconnection patterns may be realized by examining estimates of the expected correlation of time averages as computed from (5).

Acknowledgments. Helpful discussions during the course of this work with our colleagues T. L. Bell, K. M. Lau and G. R. North are gratefully acknowledged.

REFERENCES

Bell, T. L., 1982: Optimal weighting of data to detect climatic change. *J. Geophys. Res.*, **87,** 11 161–11 170.

Cahalan, R. F., 1981: Simple stochastic cloud dot models useful in interpreting satellite data. *Preprints 7th Conf. Probability*

and Statistics in the Atmospheric Sciences, Monterey, Amer. Meteor. Soc., 44–46.

——, D. A. Short and G. R. North, 1982: Cloud fluctuation statistics. *Mon. Wea. Rev.*, **110,** 26–43.

Gruber, A., and J. S. Winston, 1978: Earth-atmosphere radiative heating based on NOAA scanning radiometer measurements. *Bull. Amer. Meteor. Soc.*, **59,** 1570–1573.

Hasselmann, K., 1979: On the signal-to-noise problem in atmospheric response studies. *Meteorology Over the Tropical Oceans,* D. B. Shaw, Ed., Roy. Meteor. Soc., 251–259.

Heddinghaus, T. R., and A. F. Krueger, 1981: Annual and interannual variations in outgoing longwave radiation over the tropics. *Mon. Wea. Rev.*, **109,** 1208–1218.

Horel, J. D., and J. M. Wallace, 1981: Planetary scale atmospheric phenomena associated with the Southern Oscillation. *Mon. Wea. Rev.*, **109,** 813–829.

Jones, R. H., 1975: Estimating the variance of time averages. *J. Appl. Meteor.*, **14,** 159–163.

Lau, N-C., 1978: On the three-dimensional structure of the observed transient eddy statistics of the Northern Hemisphere wintertime circulation. *J. Atmos. Sci.*, **35,** 1900–1923.

Leith, C. E., 1973: The standard error of time-average estimates of climatic means. *J. Appl. Meteor.*, **12,** 1066–1069.

Liebmann, B., and D. L. Hartmann, 1982: Interannual variations of outgoing IR associated with tropical circulation changes during 1974–78. *J. Atmos. Sci.*, **39,** 1153–1162.

Madden, R. A., 1976: Estimates of the natural variability of time-averaged sea-level pressure. *Mon. Wea. Rev.*, **104,** 942–952.

——, 1981: A quantitative approach to long-range weather prediction. *J. Geophys. Res.*, **86,** 9817–9825.

——, and D. J. Shea, 1978: Estimates of the natural variability of time-averaged temperature over the United States. *Mon. Wea. Rev.*, **106,** 1695–1703.

Reed, R. J., 1979: Cyclogenesis in polar air streams. *Mon. Wea. Rev.*, **107,** 38–52.

Short, D. A., and J. M. Wallace, 1980: Satellite-inferred morning-to-evening cloudiness changes. *Mon. Wea. Rev.*, **108,** 1160–1169.

Wallace, J. M., and D. S. Gutzler, 1981: Teleconnections in the geopotential height field during Northern Hemisphere winter. *Mon. Wea. Rev.*, **109,** 784–812.

White, G. H., 1982: An observational study of the Northern Hemisphere extratropical summertime general circulation. *J. Atmos. Sci.*, **39,** 24–40.